Proc. of International Conference on Silicon Dielectric Interfaces, Research Triangle Park, NC 25-27 February 2000.

Near-Field Scanning Optical Microscopy as an Imaging Tool for Silicon Carrier Processes

H. D. Hallen [a] and A. H. La Rosa [b]

[a] *Department of Physics, NC State University, Raleigh, NC 27695-8202*

[b] *Department of Physics, Portland State University, Portland, Oregon 97207*

Characteristic time variations of carrier processes, such as the recombination of excess carriers, of oxidized silicon are measured as a function of position using near-field scanning optical microscopy (NSOM). Typical time constants from the region imaged agree well with those obtained by conventional spatial-averaging techniques for a wide range of samples. Images locate defects, reveal variations, and can map the regions in which a particular recombination process is active. The technique will be reviewed including the limits of resolution and signal strength, with illustrations from a variety of samples. Carrier diffusion in confined layers, such as SOI samples, will be discussed.

I. INTRODUCTION

Time-resolved optical semiconductor characterization techniques with fine spatial resolution offer a unique opportunity to study the dynamics of carriers. We have developed such a technique by exploiting standard infrared carrier lifetime measurement methods in a near-field scanning optical microscope (NSOM). Subwavelength spatial resolution is provided by the NSOM,[1, 2] and the time-resolved sensitivity allows one to map carrier lifetime as a function of position. The technique can be used to locate any defects that reduce that lifetime locally.[3-6] It results in a map of carrier dynamics that identifies the dominant processes as a function of position on the sample.[7]

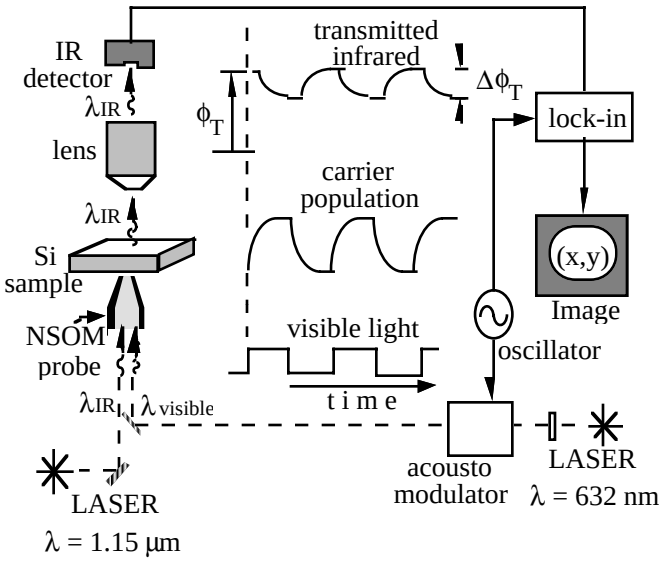

Figure 1 Schematic of the experiment that extracts information about the local dynamics of excess carriers in a semiconductor. Left side : optical path of the IR radiation through the microscope. Center: A timing diagram of the process. The visible light creates carriers which decay over their lifetime. An increase in carriers causes a decrease in the IR transmission. Right : Diagram of the synchronous detection of the transmitted infrared signal. An image is constructed as the probe is scanned across the sample.

II. EXPERIMENT

An NSOM achieves sub-wavelength resolution by geometrically confining light within a small aperture that is placed in close proximity to the sample. Resolution is a function of the physical size of the aperture and the distance between that aperture and the sample surface, not by the wavelength of the light employed. The sharpened optical fiber is coated with metal by rotating the probe with the tip angled away from the evaporation source so that an aperture is left uncoated. We have used fibers sharpened by the heat-and-pull method[8] and by etching.[9] Aluminum forms the aperture. The probe is positioned near the surface under lateral force feedback.[10-12] The NSOM is used in illumination mode, with 1.15 μm

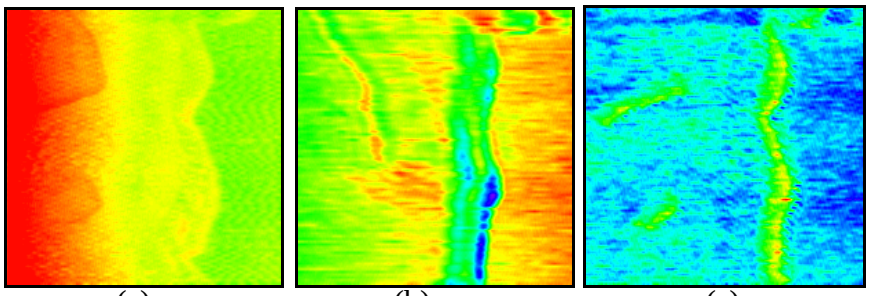

(a) (b) (c)

Figure 2: Three images show the same 20 micron square region of an oxygen terminated silicon surface with different contrast methods. (a) A topographic image of the region shown with a 240 nm vertical rainbow range and with red higher. (b) The infrared transmission (0.44 nW range with a ~80 nW dc background subtraction) shows regions of contrast, red more intense, near some of the multiple step defects and on some terrace areas. (c) The time-resolved image of IR amplitude change while the visible light is switched reveals regions near part of the multiple step defects which have a faster recombination rate (green). The range is 0.038 nW.

HeNe laser light and either 514 nm Ar ion or 632 nm HeNe laser light coupled into the back of the fiber probe. The primary difficulty encountered in NSOM-Raman is that of low signal levels. Input of more than a few milliwatts of light into the probe's fiber will destroy the probe tip.[13] Smaller tip apertures strongly reduce the probe throughput.[14] A schematic of the microscope and detection geometry (with the tip greatly enlarged) is shown in the left side of Figure 1.

Carrier lifetime (τ) is defined as the average time excess carriers exist within a sample before they recombine and are thereby annihilated. During that time they contribute to the conductivity of a sample and may be collected in a device such as a photodetector. In our experiment,[4] visible laser light is modulated to create a time-varying excess carrier distribution (Figure 1). This distribution is monitored by noting its effect on continuous wave infrared (IR) laser radiation also illuminating the sample. The photo-excited carriers scatter the IR light thereby reducing its intensity at the detector. Both visible and IR light are brought to the sample through the same NSOM probe aperture. This configuration insures high lateral resolution and avoids mismatch in the sample regions illuminated by either laser light. We record the change in the transmitted IR signal, $\Delta\phi_T$, as the visible light is switched on and off, using a lock-in amplifier as shown in figure 1. The magnitude of the change in the IR signal at a given visible light switching frequency is related to the lifetime. The samples used in these studies were oxidized silicon.

III. RESULTS AND DISCUSSIONS

An example of this imaging technique is shown in Figure 2. On the left is the topography, in the center the IR transmission with the visible light off, and at the right the IR variation as the visible light is switched (related to carrier lifetime). Note that the carrier lifetime is reduced near some of the topographic steps seen in (a), as expected since steps are defects. One can learn more by varying the frequency of the visible switching light. When the visible light frequency is slow compared to the carrier lifetime, equilibrium is reached during each light cycle, and the DIR signal is maximized. At high frequencies, the carrier population cannot respond and the signal decreases. This is shown in Figure 3(a) for two different samples with widely disparate lifetimes. The knees on the plots relate directly to the lifetime. We can image at any visible switching frequency. The remainder of Figure 3 illustrates some examples from the lower recombination rate sample of Figure 3(a). The images below and above the recombination rate are very different, as expected since the lower frequency image contrast is dominated by carrier recombination while the higher frequency data are dominated by a higher rate serial process -- carrier diffusion. Note that the higher frequency images are similar. This is expected since they image the same process. The only reason why they are different at all is that the images at a few kHz still contain some contrast from the tail of the carrier lifetime response. The small-scale structure is not noise, but relates to the small size of the defects with ~100nm resolution. The resolution is given by the aperture size combined with the probe to silicon surface distance, which is limited by the 60nm thick oxide on this surface.

Using this technique it is possible to produce quantitative data in addition to qualitative high resolution images. This is accomplished by noting the cross-over (knee) frequency. We have compared the lifetime measured as the inverse of the knee frequency (a local measurement) to the average lifetime measurement for the entire sample using an independent method. We find agreement between the our local method and the large-area technique for samples with lifetimes as different as 10 μs and 1.6 ms.[4, 7]

At first glance it seems unlikely that we could obtain ~100 nm resolution for processes on such a long time scale given the mobility of the carriers in silicon. Indeed, the diffusion coefficient in crystalline silicon is $D=10\ cm^2/s$ and within a (short) lifetime of just one microsecond, the diffusion length $(D\tau)^{1/2} \approx 30\ \mu m$ is much greater then the size of images. Therefore, the mobile carriers concentration at certain point is determined by relaxation rates in an extensive surrounding domain. Nevertheless, as our data demonstrate and a simple argument below corroborates, detectable variations are observable due to changes in a local area, much smaller then $(D\tau)^{1/2}$. In fact, one can provide a very simple heuristic argument for a simplified case of a spherical region of radius R with zero lifetime within and no recombination outside. The exact solution is proportional to (1 - R/r), suggesting that this limit to resolution depends upon the feature size R and not the diffusion length. The resolution on our samples is limited by the probe and geometry, since the defects are very small.

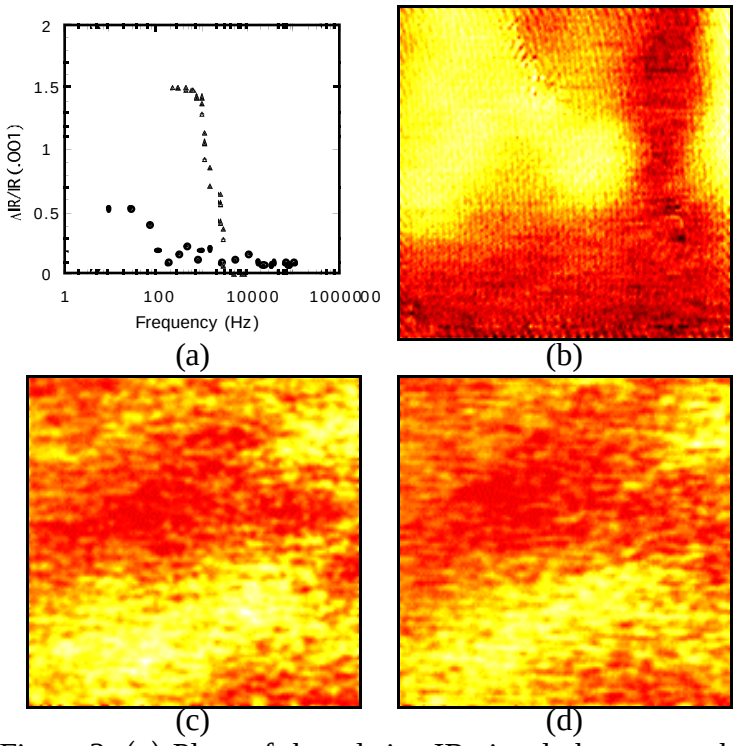

Figure 3: (a) Plots of the relative IR signal change vs. the visible light switching frequency are shown for two different samples. The samples with data as triangles and circles have effective lifetimes estimated from the knee of 20 msec and 1.6 msec, respectively. (b)-(d) The effects of varying the visible light switching frequency in 7.5 mm square images of nearly the same area on the 'circle' sample(white high, red, black low). (b) An image of the IR signal change as the visible light is switched on and off at 100 Hz with 0.27 nW range. (c) As (b), but at a frequency of 2 kHz, 0.03 nW range. (d) At 20 kHz modulation, 0.03 nW range.

The images shown in Figure 4 correspond to the same scanned area, a $(7.5\ \mu m)^2$ square, of a silicon-on-insulator (SOI) sample. We present the topography and the IR transmission image for comparison, and time-resolved images taken at several visible modulation frequencies. The topography reflects surface height variations due to variations of the silicon thickness or surface layers. We see that, for this region of the sample, the time-resolved images are almost independent of the visible modulation frequency and correlate to the IR transmission image. It is quite unlike the data in Figure3 and also unlike other regions of the sample that showed less topographic variation. We can understand this in the following simple model: Since the absorption coefficient of green light (λ = 514 nm) in silicon is $\alpha \sim 10^4\ cm^{-1}$ (light penetrates up to $\Delta z \sim 1\ \mu m$), there should be a strong influence of silicon thickness variation on the optical signals. It should be true for both the average (transmission) and time resolved signals. Further, the diffusion of carriers from beneath the probe is limited to the thickness of the silicon, so variations in the thickness of the silicon layer would induce contrast in the steady-state carrier density. This effect influences both the IR and pulsed measurements. It seems that these geometric considerations dominate over the contribution from carrier lifetime modulation in this sample region. Thus the contrast

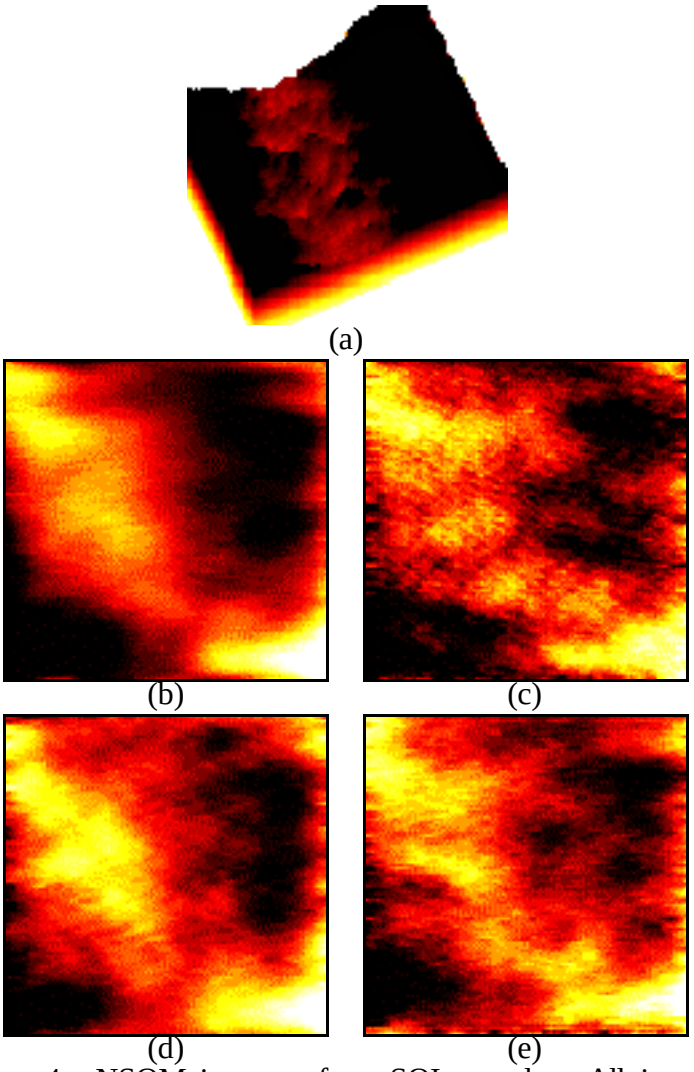

Figure 4: NSOM images of an SOI sample. All images correspond to the same region of 7.5 μm x 7.5 μm. (a) Sample topography derived from a shear-force feedback (the gray scale range is 15 nm - black higher). (b) The infrared transmitted intensity as a function of position with 0.3 nW range (white higher) and a 5 nW background subtracted. (c-e) The time-resolved images taken at the following frequencies, RMS range: (c) 170 Hz, 6.2 pW, (d) 750 Hz, 4.5 pW, and (e) 8.5 kHz, 2.5 pW. A strong influence of the transmitted infrared signal is observed in the time-resolved images, although the resolution varies. Topographic image reveals that the thickness of either top Si or buried oxide or both vary across the analyzed region.

observed in the transmission image should be interpreted primarily in terms of thickness variations. The IR transmitted signal indicates $\Delta\phi_T / \phi_T = 6 \times 10^{-2}$. Since $\phi_T \sim \exp(-\alpha z)$, a Δz thickness variation should induce a signal change of $\Delta\phi_T / \phi_T = \alpha \Delta z$. From here we obtain $\Delta z \sim 60$ nm, a value that is in agreement with the order of magnitude changes of the topographic image.

IV. CONCLUSIONS

In conclusion, we have successfully imaged the spatial distribution associated with carrier processes possessing different lifetimes. The spatial resolution is given by a combination of the NSOM probe, the signal level, and the effects of diffusion, which tend not to decrease the contrast of the image. We have shown that the local lifetime measurements taken in an NSOM compare well with the spatial-averaging techniques widely used. Finally, we point out that diffusion and absorption length changes must be taken into account when surface topography indicates variations of silicon thickness in silicon on insulator samples.

ACKNOWLEDGEMENTS

We would like to thank Gerry Lucovsky for useful discussions and encouragement during the course of this work and indeed for all the time we have been at NCSU. Gerry has taught us what it means to be a leader, a manager, a scientist, and an atom bonded into a solid. His insights into the actual configuration of the silicon-silicon dioxide interface and broad background in carrier processes have contributed to the quality of this work. This work was supported by the U.S. Army Research Office through grants DAAH04-95-1-0380 and DAAH04-93-G-0194.

1. Betzig, E. and J.K. Trautman, *Near-field optics: Microscopy, spectroscopy, and surface modification beyond the diffraction limit.* Science, 1992. **257**: p. 189-195.
2. Pohl, D.W., W. Denk, and M. Lanz, *Optical stethoscopy: Image recording with resolution λ/20.* Applied Physics Letters, 1984. **44**(7): p. 651-653.

3. LaRosa, A., C.L. Jahncke, and H.D. Hallen, *Time as a contrast mechanism in near-field imaging.* Ultramicroscopy, 1995. **57**: p. 303-308.
4. LaRosa, A.H., C.L. Jahncke, and H.D. Hallen, *Time-resolved contrast in near-field scanning optical microscopy of semiconductors.* SPIE Proceedings, 1995. **2384**: p. 101-108.
5. LaRosa, A.H., B.I. Yakobson, and H.D. Hallen, *Imaging of Silicon Carrier Dynamics with Near-field Scanning Optical Microscopy.* Mater. Res. Soc. Symp. Proc., 1995. **406**: p. 189-194.
6. Hallen, H.D., A.H.L. Rosa, and C.L. Jahncke, *Near-field scanning optical microscopy and spectroscopy for semiconductor characterization.* Phys. Stat. Sol. (a), 1995. **152**: p. 257-268.
7. LaRosa, A.H., B.I. Yakobson, and H.D. Hallen, *Optical Imaging of Carrier Dynamics with Subwavelength Resolution.* Appl. Phys. Lett., 1997. **70**(13): p. 1656-1658.
8. Yakobson, B.I., P.J. Moyer, and M.A. Paesler, *Kinetic limits for sensing tip morphology in near-field scanning optical microscopes.* J. Appl. Phys., 1993. **73**(11): p. 7984-7986.
9. Hoffmann, P., B. Dutoit, and R.-P. Salathé, Ultramicroscopy, 1995. **61**: p. 165.
10. Betzig, E., P.L. Finn, and J.S. Weiner, *Combined shear force and near-field scanning optical microscopy.* Applied Physics Letters, 1992. **60**(20): p. 2484-2486.
11. Toledo-Crow, R., *et al.*, *Near-field differential scanning optical microscope with atomic force regulation.* Applied Physics Letters, 1992. **60**: p. 2957.
12. Karrai, K. and R.D. Grober, *Piezoelectric tip-sample distance control for near-field optical microscopes.* Applied Physics Letters, 1995. **66**(14): p. 1842.
13. LaRosa, A.H., B.I. Yakobson, and H.D. Hallen, *Origins and effects of thermal processes on near-field optical probes.* Appl. Phys. Lett., 1995. **67**(October 30).
14. Yakobson, B.I. and M.A. Paesler, *Tip optics for illumination NSOM: Extended zone approach.* Ultramicroscopy, 1995. **57**: p. 204.